

## **MODIFYING GELDART CLASSIFICATION FOR VARIOUS COHESION FORCES**

**Tal Yehuda<sup>2</sup> and Haim Kalman<sup>1,2</sup>**

1. *Aaron Fish Chair in Mechanical Engineering – Fracture Mechanics*
2. *Lab for Conveying and Handling of Particulate Solids, Department of Mechanical Engineering, Ben-Gurion University of the Negev, Beer Sheva 8410501, Israel  
Talyehu@post.bgu.ac.il*

Fluidized beds (FB) have significant applications in various industries. Classical Geldart classification is used for a long time to classify materials to four groups, each behave differently in a fluidized bed. Geldart's classification is based on the relationship between the particle and fluid density difference and the particle diameter. The four groups show behavior related to the cohesion forces. Group C has very high cohesion forces to create channels or rising plugs. Group A has countable cohesion forces while particles behave as individuals to present a bed volume increase at fluidization. Groups B and D are big enough to have negligible cohesion forces show none of the above – fluidization starts as bubbling and slugging. However the classical Geldart classification is based on dry materials in which the major cohesion force is related to Van der Waals force. In this research the effect of other cohesion forces on the classification is examined. A number of materials were tested at various moisture contents to present cohesion forces by liquid bridges. By these tests materials originally classified in groups B or D behaved like groups C or A at various moisture contents. Further, experiments with liquid fluidization were conducted. In this case there are no liquid bridge forces and also the Van der Waals forces are negligible. Indeed, even materials originally classified to groups C or A are expected to behave like groups B or D. In this way, Geldart's classification can be modified to consider various cohesion forces.

KEY WORDS: Fluidized bed; Interparticle forces; Geldart's classification.

### **1. INTRODUCTION**

Fluidized beds, both in liquid and gas are frequently used in industry, for many different applications, Daizo and Levenspiel (1991). It can be used for drying, heating and cooling solids, as well as for mixing or separating particles which differ from each other by size or density, and also for enhancing chemical reactions usually between gas and solids, and more.

When using fluidized beds for any of the applications mentioned above it is essential to foresee and understand the beds behavior. Geldart created a chart classifying different

fluidizations by the material and fluid properties, Geldart (1973). Geldart classified the different fluid-material combinations into four groups, each group has different fluidization characteristics. The reason for the different behavior of each group is the effect of the interparticle forces, Israelachvili (2011), Rietema et al. (1993). More accurate is the magnitude of the interparticle forces to gravity ratio, Feng and Yu (2000), Seville et al. (2000), Yu et al. (2003).

This paper describes experiments conducted with both water and air fluidized bed experimental setups. The goal of this work is to investigate the effects of the interparticle forces - Van der Waals and liquid bridge forces on the fluidization characteristics. A water fluidization system and fine powders classified as C, will be used to study the effects of the Van der Waals forces, knowing that the Van der Waals forces are weaker in a water surroundings, making the bed easier to fluidize, Israelachvili (2011). For the liquid bridge forces, an air fluidization system will be used, fluidizing relatively big particles classified as D with moisture content high enough to form the bridges, finding whether they will act as type A or even type C particles under the stronger cohesive forces.

### **1.1. FLUIDIZED BED CHARACTERISTICS**

As was mentioned before, Geldart (1973) classified the different fluidizations into four groups: C – cohesive, A – aeratable, B – bubbly and D – spoutable. Geldart's chart is based on the common case of fluidizing dry particles with air, the dominant interparticle forces in this scenario are the Van der Waals forces. Type C represents very small and light particles, usually powders, it characterized as very hard to fluidize because of the high interparticle forces (Van der Waals) to gravity ratio. While increasing the fluid velocity the fluid pressure drop over the bed increases, as a result a couple of phenomena may occur: creation of channels inside the packed bed of particles or plugs of material rising to the top of the bed. Type A represents particles slightly larger in size or density or both than C, so the interparticle forces are still affecting but not as dominant as they are for type C particles. Reaching the minimum fluidization velocity in a type A bed of particles results in a small increase in the bed height, right before the bubbly fluidization take place. The particles change of configuration is the outcome of the cohesive forces between the particles and the increase in pressure drop over the bed. Further increasing the velocity results in a bubbly fluidization followed by a sluggish fluidization. For particles type B and D after the stationary state the bed will be bubbly fluidized without a change in the bed's height in between, with further increase in gas flow rate the fluidization will become sluggish, Shaul et al. (2012), Shaul et al. (2013).

For liquid fluidized bed, the fluidization characteristics are a little different, mainly because the liquid density and viscosity are much higher than air. For most materials when reaching the minimum fluidization velocity, the bed will start expanding smoothly without any large scale voids, the phenomenon is usually referred to as homogenous fluidization. A bubbly fluidization will occur rarely, only for a combination of high density particles with low density liquids, Daizo and Levenspiel (1991) Felice (1995), Mandal (2015).

## 1.2. INTERPARTICLE FORCES

There are several interparticle forces, as was mentioned before, this study focuses on two: Van der Waals forces, and liquid bridge forces.

The Van der Waals forces have an important role in phenomena involving interparticle forces, because they always exist. The Van der Waals forces arises between atoms and molecules due to charge interactions, among them are dipole-dipole, dipole-induced dipole and dispersion forces. Generally a particle in the size of 100 $\mu\text{m}$  or less, will be affected by the force, Seville et al. (2000).

A simplified equation for calculating the forces between two spheres was given by Yu et al. (2003):

$$F_v = \frac{AR}{12a^2} \quad (1)$$

where  $R$  is the radius of the sphere,  $a$  is the separation distance and  $A$  is the Hamaker constant. It is easy to notice in equation (1) that the force is more sensitive to separation distance than the particle size. The Hamaker constant which is material and medium related, is the reason for the decay of the forces in water versus air, Israelachvili (2011).

Another cohesive force is the liquid bridge force (see Fig. 1). Adding liquid to the solid particles creates liquid bridges between the particles. The liquid bridge increase particles attraction. The force exhibits both dynamic and static forces and composed of three components: The surface tension force, the Laplace pressure deficiency and the liquid viscous forces, the latter does not apply in our case as we are interested in the static components, Pepin et al. (2001), Seville et al. (2000) and Yu et al. (2003), offer similar ways to calculate the liquid bridge force, the way described ahead is both simple and efficient:

$$F_l = 2\pi r_2 \sigma + \pi r_2^2 \Delta P \quad (2)$$

where  $\sigma$  is the surface tension and  $\Delta P$  is the Laplace pressure deficiency. In order to calculate the Laplace pressure deficiency:

$$\Delta P = \sigma \left[ \frac{1}{r_1} - \frac{1}{r_2} \right] \quad (3)$$

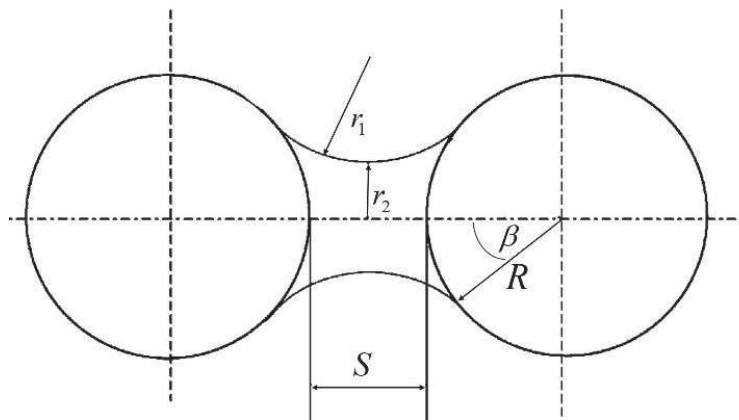


Fig.16 Liquid bridge between two equal

$r_1, r_2$  are the curvature radii and can be calculated as follow:

$$\begin{aligned} r_1 &= R[(1+h)\sec\beta - 1] \\ r_2 &= R[1 + (1+h)\tan\beta - (1+h)\sec\beta] \end{aligned} \quad (4)$$

where  $h$  is the relative surface gap between particles, and  $\beta$  is the filling angle. For water the liquid bridge force is larger in magnitude than the Van der Waals force, moreover it differ from it by the option to alter the force magnitude and properties, by altering the liquid's amount or replacing it with another, Pepin et al. (2001).

## 2. EXPERIMENTAL

Table 1 lists the nine materials tested in the conducted experiments. For the air fluidization the materials were classified as D and the sand for the water was classified as C. The results for the sand in water will be presented in the presentation. The mean particle size ranges from 0.014 to 4.5 mm and particle density ranges from 954 to 5964  $kg / m^3$ . The bed height for all the experiments was about 18 cm in an 81 mm diameter pipe.

Table 1

Experimental materials					
Material	Particle mean size $d_{sv}$ mm	Particle density $\rho_p$ $kg / m^3$	$Ar$ – Archimedes number	Geldart's group	Fluidization fluid
Alumina	0.875	1653	37,500	D	Air
Glass	0.875	2600	59,000	D	Air
Green zirconium	2.1	5964	1,870,000	D	Air
Olive waste	2.2	1133	408,000	D	Air
Plastic	4.5	954	2,940,000	D	Air
Sand	1	2600	88,100	D	Air
wheat	3.2	1251	1,390,000	D	Air
Zirconium	0.75	5964	85,200	D	Air
Sand	0.014	2500	0.0038	C	Water

Figures 2 and 3 illustrates the water fluidized bed system and the air fluidized bed system, respectively. The water circulating in the liquid fluidized bed setup is preserved in a plastic tank (1) at ambient conditions. The water is being pumped out of the tank by a centrifugal pump (2). In order to control the water flow rate the bypass (3) and the main line valve (4) are being used combined. The water continues to the electromagnetic flow rate meter (5). Before entering the experimental pipe, the water goes through the distributor (6), the distributor is a packed bed of plastic pallets followed by a fiber filter.

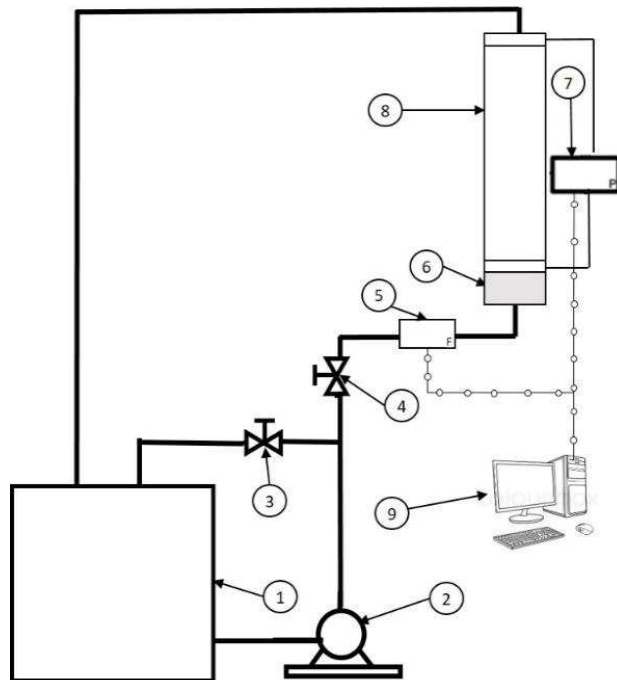


Fig. 2 Scheme of the water experimental system.

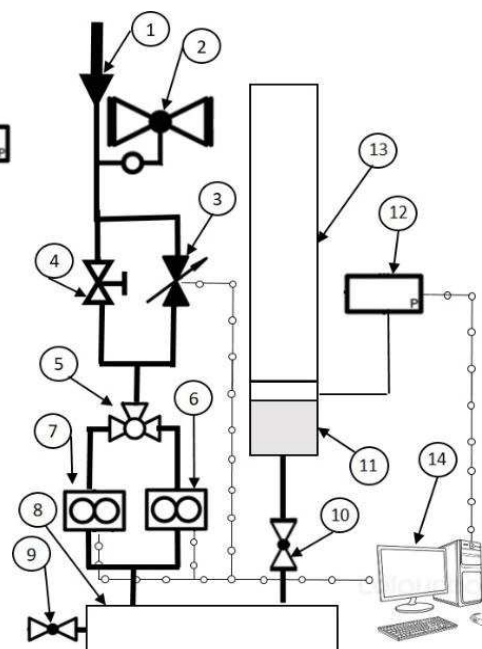


Fig.3 Scheme of the air experimental system.

The experimental pipe (8) is made of glass, its diameter is 81 mm and its length is 1m. The water pressure drop over the bed is measured by the pressure transducer (7), through two measuring points one under the experimental pipe and one over it as illustrated. The water departing from the experimental pipe circulate back to the tank. The data measured was acquired by a LabVIEW acquisition system (9).

The experiment procedure is simple. First the pipe is being filled by the particles, the dry bed height is measured, than it is filled with water, it is important to make certain that all the air left the system. After the bed is fully wet and the system is filled with water the experiment starts using valves (3) and (4) to slowly increase the water flow rate, after reaching the maximum flow rate for the experiment, the flow rate is slowly decreased until it is back to zero. Producing the pressure drop over the bed vs. the water superficial velocity curve. The air provided to the air fluidization system is dry air at 5°C with a constant source pressure of 5 bar, the air enters the system via the main air support pipeline (1). The air is than reduced to 3 bar by a pressure regulator (2). The air continues through the manual valve (3) or the more accurate PC controlled valve (4). With the three way plug valves (5) it is possible to divert the air flow between the two thermal mass flow rate meters (6) and (7). The air then flows into the air tank (8), by opening the valve (10) the air flows into the experimental pipe, opening (9) discharges the air from the tank (9). Before the air enter the experimental pipe (13) it goes through the distributor (11) which are both identical to the ones in the liquid setup. The air pressure drop over the bed is measured from just above the distributor to the ambient (12).

All the data was acquired by a LabVIEW acquisition system (14). The air fluidization experiments were performed as follows: a day or more before conducting the experiment, the material being studied was wetted to the desirable moisture content, it was performed

by checking the weight of the material and mixing it with the right amount of water. Before mounting the experimental pipe slowly with the moist material, the material is being checked for its moisture content with the Moisture Analyzer device, after carefully mounting the pipe the beds height is being measured. At this point the fluidization begins, the material is being fluidized several times until it is completely dry. Each fluidization ends after a sufficient amount of time, in which it is possible to determine which of the Geldart's classification groups is suitable to characterize the fluidized bed, according to the visible bed behavior and its fluidization curve (the air pressure drop over the bed vs. the air velocity). In each fluidization the bed moisture content was measured two times, at the top of the air velocity and after the velocity was decreased back to zero, during the experiments the air velocity was increased and decreased gradually.

All the data measured for both experimental setups was exported to the Excel for further analysis.

### 3. RESULTS AND DISCUSSION

As was mentioned in the previous chapter two types of experiments were conducted, one with water and one with air as the fluidizing fluid, the analysis starts with the latter.

The results of one experiment conducted on sand particles is presented in Fig. 4, the figure shows the fluidization curves of the sand as it is drying while fluidizing. The moisture content of the sand in the beginning of each fluidization is also presented next to the curve. As seen in the fluidization curves and by observing the bed behavior, as the wet sand dried its classification according to its fluidizing characteristics changes, it starts at type C (fluidizations A-E), through type A (fluidization F) to type D (fluidization G) when the sand is completely dry.

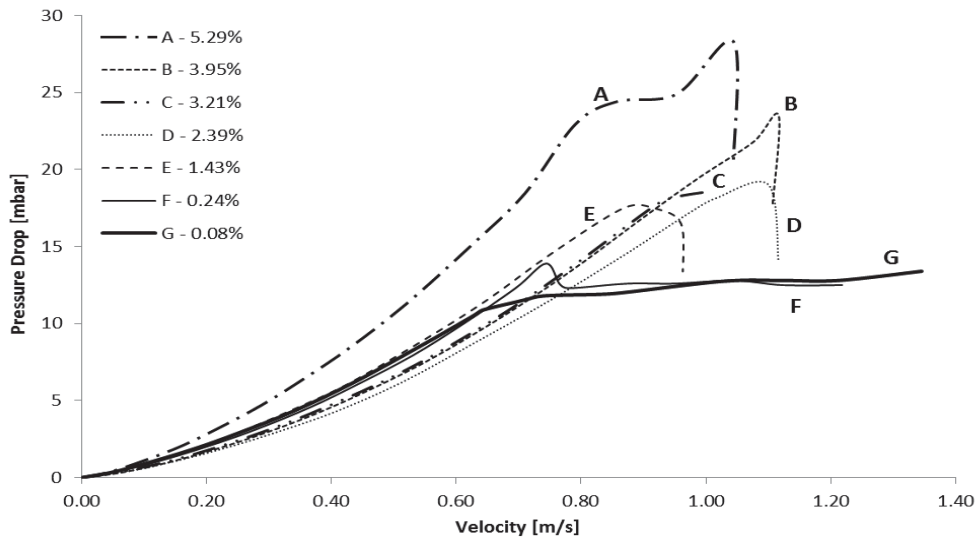


Fig.4 The pressure drop across a fluidized bed of sand particles vs. the rising air velocity, with moisture content of 5.29% for fluidization 'A' down to 0.08% for fluidization 'G'.

After experimenting with all the subjected materials it is safe to say that there is a clear connection between the surface moisture content and the fluidization characteristics. The moisture content presented in Fig. 4 is defined in this paper as:  $\text{water}/(\text{water} + \text{dry solid})$ .

For the sake of comparing different particles with different porosities, the moisture content alone is not sufficient, knowing that only the liquid on the surface creates the liquid bridges – the cohesive forces which affect the bed behavior, porous particles may absorb the liquid so it does not take part in creating the bridges. Further, the absorbed liquid increases the particles density which already classified as D. In order to determine the amount of liquid on the surface, further analysis was required. During each experiment the bed moisture content was examined by taking a sample out of the bed and deploying it to the Moisture Analyzer, the Moisture Analyzer heats the material in a pre-set temperature, in this experiment 150°C, every second while heating it returns the sample's weight until it is completely dry. Fig. 5 shows the normalized drying sand curve. According to Chandran et al. (1990), Davidson et al. (2001) and Park et al. (2003), the part from the beginning of the curve until point B is the constant rate drying period, it relates to the moisture content on the surface. From point B and on it is the falling rate drying period which relates to the internal diffusion. Point A represents the time it took the device to heat up to 150°C. A simple analysis of the curve gives us a surface moisture content of 70% of the total moisture content.

Several water fluidization experiments were conducted. At the start of the fluidizations, the bed particles had to be wetted entirely, the water molecules flowing from the distributor beneath the bed wetted the coarse particles easily, but, because of the strong cohesive Van der Waals forces, it needed external mixing to get the fine particles entirely wetted. After it was fully wet, the water fluidized the bed in all the experiments conducted, the fluidization characteristics were as expected according to the literature. Increasing the water's velocity resulted in a relatively sharp rise in the fluidization curve for the fixed bed, when reaching the critical fluidization velocity the bed started expanding with the rise in water velocity, while the fluidization curve trend turned moderate, almost horizontal.

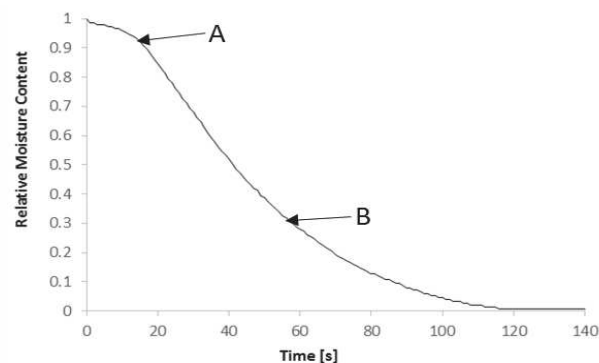


Fig.5 The moisture content while heating normalized by the total moisture content of the experimented sand.

#### 4. CONCLUSIONS

Using two experimental systems, one for air fluidized bed and one for water fluidized bed, this research examines the effect of liquid bridge forces on the air fluidized bed characteristics, and the effect of the strong Van der Waals forces when fluidizing a powdery material inside the water fluidized bed. As for the latter, the theory suggests a regular fluidization curve and visible characteristics as for any liquid fluidized bed,

meaning that the effect of the Van der Waals forces inside the water medium will be reduced compared to the forces while fluidizing in air. The experiments conducted in the lab aligned with the theory. The results of the air fluidized bed experiments were also satisfying, it showed a clear connection between the surface moisture content to the fluidized bed characteristics. The liquid bridge forces that was created between the particles due to the surface moisture content and are stronger than the Van der Waals forces, changed the fluidization characteristics of particles normally classified as D to the fluidization characteristics of class C or A particles, it is noticeable both by observing the bed and analyzing the fluidization curve (pressure drop over the bed vs. fluids velocity).

#### ACKNOWLEDGEMENT

This research was supported by Research Grant Award No. US-4877-15 from BARD, The United States - Israel Binational Agricultural Research and Development Fund.

#### REFERENCES

1. Chandran, A. N., Rao, S. S., Varma, Y. B. G., 1990. Fluidized bed drying of solids. *AIChE Journal* 36, 29-38.
2. Daizo, K., Levenspiel, O., 1991. Fluidization engineering.
3. Davidson, J. F., Thorpe, R. B., Al-Mansoori, O., Kwong, H., Peck, M., Williamson, R., 2001. Evaporation of water from air-fluidized porous particles. *Chemical engineering science* 56, 6089-6097.
4. Felice, R.D., 1995. Hydrodynamics of liquid fluidization. *Chemical Engineering Science* 50, 1213-1245.
5. Feng, C.L., Yu, A.B., 2000. Quantification of the relationship between porosity and interparticle forces for the packing of wet uniform spheres. *Journal of colloid and Interface Science* 231, 136-142.
6. Geldart, D., 1973. Types of gas fluidization. *Powder Technology* 7, 285-292.
7. Israelachvili, J.N., 2011. Intermolecular and surface forces. Academic press.
8. Mandal, D., 2015. Hydrodynamics of particles in liquid–solid packed fluidized bed. *Powder Technology* 276, 18-25.
9. Park, Y. S., Shin, H. N., Lee, D. H., Kim, D. J., Kim, J. H., Lee, Y. K., Sim, S. J., Choi, K. B., 2003. Drying characteristics of particles using thermogravimetric analyzer. *Korean Journal of Chemical Engineering* 20, 1170-1175.
10. Pepin, X., Simons, S.J.R., Blanchon, S., Rossetti, D., Couarraze, G., 2001. Hardness of moist agglomerates in relation to interparticle friction, granule liquid content and nature. *Powder Technology* 117, 123-138.
11. Rietema, K., Cottaar, E. J. E., Piepers, H. W., 1993. The effects of interparticle forces on the stability of gas-fluidized beds—II. Theoretical derivation of bed elasticity on the basis of van der Waals forces between powder particles. *Chemical Engineering Science* 48, 1687-1697.
12. Seville, J.P.K., Willett, C. D., Knight, P. C., 2000. Interparticle forces in fluidisation: a review. *Powder Technology* 113, 261-268.
13. Shaul, S., Rabinovich, E., Kalman, H., 2012. Generalized flow regime diagram of fluidized beds based on the height to bed diameter ratio. *Powder technology* 228, 264-271.
14. Shaul, S., Rabinovich, E., Kalman, H., 2014. Typical fluidization characteristics for Geldart's classification groups. *Particulate Science and Technology* 32, 197-205.
15. Yu, A. B., Feng, C. L., Zou, R. P., Yang, R. Y., 2003. On the relationship between porosity and interparticle forces. *Powder Technology* 130, 70-76